

Effect of annealing temperature on structural and optical properties of Cr₂O₃ thin films by PLD

Mahdi Hasan Suhail¹, Souad G. Khaleel², Hawraa Kamil²

¹Department of Physics, College of Science, University of Baghdad

²Department of Physics, College of Sciences for Women, University of Baghdad

E-mail: mhsuhail@yahoo.com

Abstract

In the present work, pulsed laser deposition (PLD) technique was applied to a pellet of Chromium Oxide (99.999% pure) with 2.5 cm diameter and 3 mm thickness at a pressure of 5 Tons using a Hydraulic piston. The films were deposited using Nd: YAG laser $\lambda = (1064)$ nm at 600 mJ and 400 number of shot on a glass substrate, The thickness of the film was (107 nm). Structural and morphological analysis showed that the films started to crystallize at annealing temperature greater than 400 °C. Absorbance and transmittance spectra were recorded in the wavelength range (300-1100) nm before and after annealing. The effects of annealing temperature on absorption coefficient, refractive index, extinction coefficient, real and imaginary parts of dielectric constant were also study. It was found that all these parameters decrease as the annealing temperature increased to 500 °C, while the energy gap after annealing increase from 3.4 eV to 3.85 eV.

Key words

Pulsed Laser Deposition (PLD), Cr₂O₃, thin films, X-ray diffraction, optical band gap.

Article info.

Received: Jan. 2018

Accepted: Feb. 2018

Published: Jun. 2018

تأثير التلدين على الخواص التركيبية و البصرية لاغشية اوكسيد الكروم المحضره بطريقة

الليزر النبضي

مهدي حسن سهيل¹، سعاد غفوري خليل²، حوراء كامل بدر²

¹قسم الفيزياء، كلية العلوم، جامعة بغداد

²قسم الفيزياء، كلية العلوم للبنات، جامعة بغداد

الخلاصة

حضرت أغشية رقيقة من أوكسيد الكروم (99.999% نقي) باستخدام تقنية الترسيب بواسطة الليزر النبضي (النديميوم_ياك) ذات الطول الموجي 1064 نانومتر. حضر قرص من اوكسيد الكروم عند درجة حرارة الغرفة بسمك 3 مم وقطر 2.5 سم عند ضغط 5 أطنان باستخدام مكبس هيدروليكي. تم ترسيب الاغشية بتحديد طاقة الليزر 600 ملي جول، عدد النبضات (400) نبضة تم قياس السمك للاغشية (107) نانومتر. اظهرت التحليلات التركيبية ومجهر القوة الذرية ان الافلام تبدأ بـالتبلور عند درجه حراره اكبر من 400 درجة مئوية. سجل طيف الامتصاصية والنفاذية كدالة للطول الموجي ضمن المدى (300-1100) نانومتر قبل وبعد التلدين. تأثير التلدين على الخواص البصرية المتمثلة بالانعكاسية، فجوة الطاقة للانتقال المباشر المسموح، معامل الخمود، ومعامل الانكسار، ثابت العزل بجزئة الحقيقي والخيالي وجد ان جميع هذه الخواص تقل مع زيادة درجة حرارة التلدين الى 500 درجة مئوية. وزيادة فجوة الطاقة بعد التلدين من 3.4 الى 3.85 الكترون فولت.

Introduction

As an important wide band gap semiconductor, Chromium oxide

(Cr₂O₃) has many outstanding properties, such as high hardness, chemical inertness, mechanical

strength and stability. Chromium, a 1st row transition metal, forms a number of oxides (CrO_2 , CrO_3 , Cr_2O_3 , etc.), one of these oxides is Cr_2O_3 antiferromagnetic which is the only solid chromium oxide that is stable under ambient conditions [1] and thermodynamically stable at temperatures higher than 500°C [2]. This oxide has several applications in catalysis and solar thermal energy collectors [2] hydrogen storage, wear resistance materials, dye and pigment, advanced colorants, digital recording system, black matrix films, solar energy application, coating materials for thermal protection, and electrochromic material [3]. A wide variety of chemical and physical methods have been used for large area synthesis of Cr_2O_3 films, e.g. chemical vapour deposition (CVD) at either atmospheric or low pressure, plasma enhanced CVD (PECVD), electrodeposition, metal oxidation, chemical spray pyrolysis, RF magnetron sputtering, molecular beam epitaxy and atomic layer deposition [4].

use this search method pulsed laser deposition for wide uses, and the first to use the technique of pulsed laser deposition (Smith and Turner) in 1965 where he prepares semiconductors and thin film of insulation [5].

In the present investigation, we report the effect of annealing

temperature on Cr_2O_3 thin films prepared by pulsed laser deposition in order to study the structural (XRD, AFM) and optical constants (including refractive index, extinction coefficient, real and imaginary part of dielectric constant).

Experimental

Chromium Oxide powder (99.999% pure) Table 1 shows material properties of Cr_2O_3 , was compacted into a pellet of 2.5 cm diameter and 3 mm thickness at pressing it under 5 Tons using a Hydraulic piston. Films have been deposited onto glass substrate from Cr_2O_3 target method using pulsed laser deposition (using Nd: YAG Laser at the wavelength of 1064 nm). Laser pulse frequency was 6 Hz, the distance between the target and the substrate (with dimensions of 2.5 cm \times 2.5 cm) was 6.5 cm at 600 mJ and 400 numbers of shot. Schematic diagram of a pulsed laser deposition system is shown in Fig.1.

Table 1: Material properties of Cr_2O_3 [6].

Molecular formula	Cr_2O_3
Molar mass	151.9904 g/Mol
Appearance	Light to dark green
Density	5.22 g/cm ³
Refractive index	2.551
Boiling point	4000 °C
Melting point	2435 °C
Crystal structure	Hexagonal

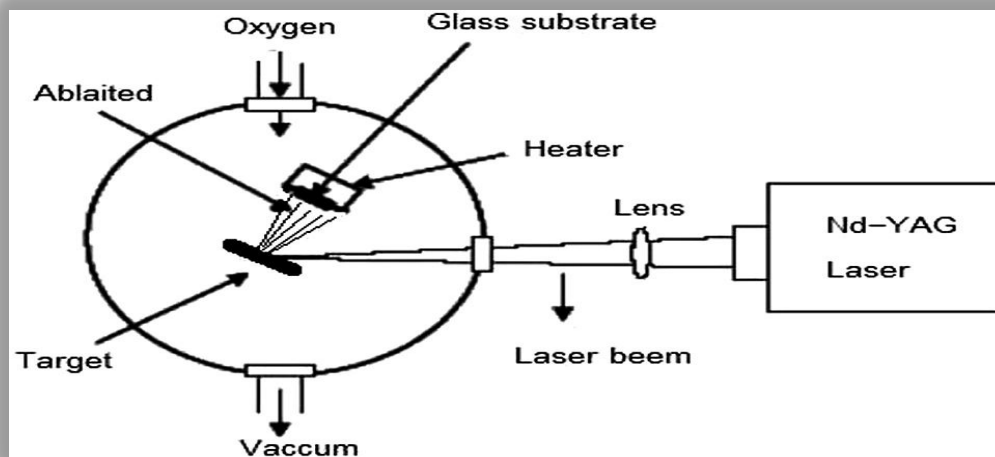


Fig. 1: Schematic diagram of pulsed laser deposition system.

The base pressure inside the chamber was typically low pressure (8×10^{-2} mbar) and a vacuum chamber generally at (10^{-3} Torr). The laser beam passed variable beam attenuator and was focused onto the target inside a chamber under 45° angle. The glass substrates have been first cleaned in detergent and water to remove any oil or dust that might be attached to the surface of the substrate, and then they are rubbed gently under tap (15) minutes. After that, they are placed in a clean beaker containing distilled water and then rinsed in ultrasonic unit for (15) minutes with pure alcohol solution. The slides eventually are dried by air blowing and wiped with soft paper. The thickness of the films (107 nm) was measured by the Tolansky interference method. Structural analysis of Cr_2O_3 thin films has been carried out in X-ray diffractometer type SHIMADZU, power diffraction system with CuK_α ($\lambda = 1.54056 \text{ \AA}$). The X-ray scans are performed between 2θ values of 20° and 80° . The surface morphology, particle size distribution and root mean square of roughness of films prepared under various conditions were analyzed using atomic force microscope model (AA3000 Scanning

Probe Microscope SPM, tip NSC35/AIBS from Angstrom Advance Inc). The optical absorbance spectra of Cr_2O_3 films on glass substrates under different deposition condition (number of shots and annealing temperatures) were measured using spectrophotometer (SHIMADZU UV-Visible 1650 PC), covering the wavelength range 200 - 1100 nm.

Results and discussion

1. Structural and morphological studies

Fig. 2 shows the X-ray diffraction of Cr_2O_3 thin films at different annealed temperature (300, 400, 500) $^\circ\text{C}$ prepared at 600 mJ and 400 number of shot at room temperature.

We have not found any other impurity peaks in comparison with the standard values of Cr_2O_3 bulk crystal structure Fig. 3 (card no. 96-900-8085). From the figure, at 300 $^\circ\text{C}$ there is no noticeable peak in the entire range, it indicates that the films are amorphous in nature and this agree compatible with some researchers [5-8]. While at annealing 400 $^\circ\text{C}$ it is seen that there is only one peak in spectra. At more annealing temperature (500 $^\circ\text{C}$) more peak seen in the spectra.

The size of the crystallite (D) was determined from the XRD data using Scherrer formula [6]:

$$D = K\lambda / \beta \cos \Theta \quad (1)$$

where k is a correction factor=0.9, β : is the full width at half maximum

(FWHM) in radian and (λ) is the incident wavelength.

The increase in the high peaks with the increase of the degree of crystallization material, as well as an increase in crystalline size are shown in Table 2.

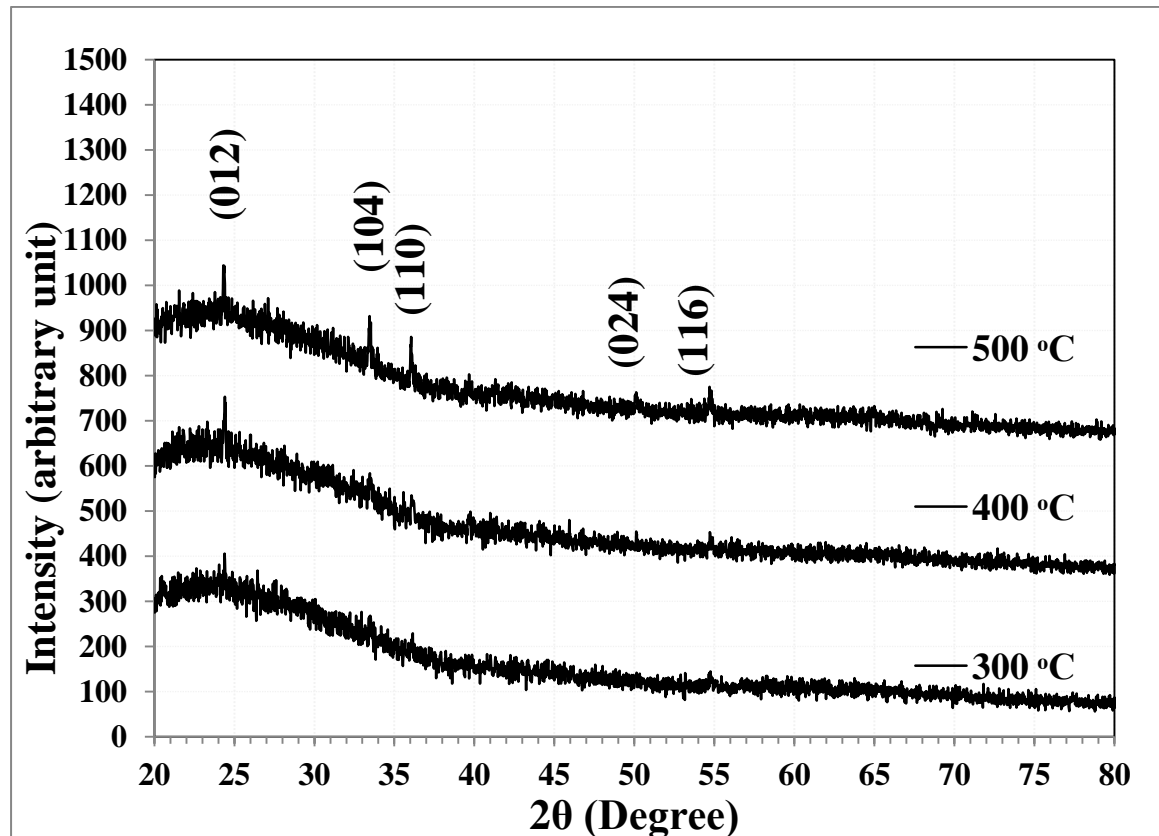


Fig. 2: X-ray diffraction of Cr_2O_3 thin films at different annealed temperature.

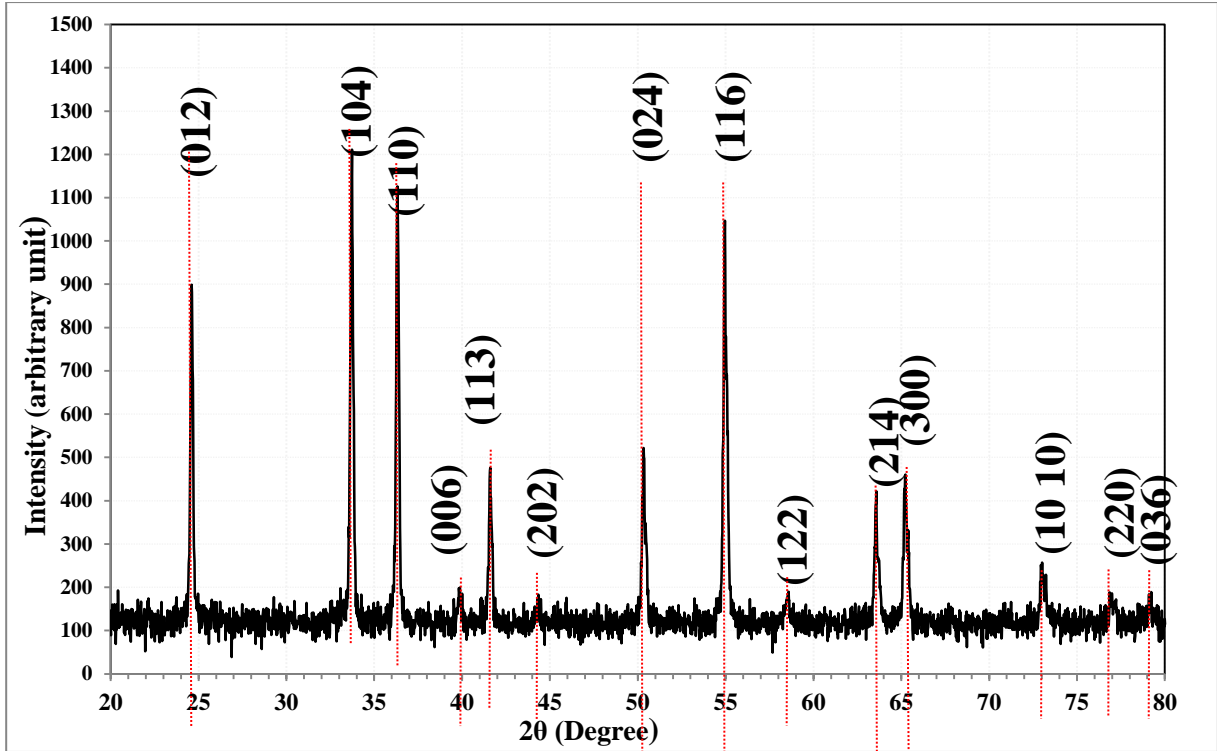


Fig. 3: X-ray diffraction of Cr_2O_3 bulk crystal structure.

Table 2: The crystalline size of the films at different annealing temperature.

T_a (°C)	2θ (Deg.)	FWHM (Deg.)	d_{hkl} Exp.(Å)	crystalline size (nm)	d_{hkl} Std.(Å)	hkl
Rt	amorphous					
300						
400	24.3875	0.2849	3.6469	28.5	3.6319	(012)
500	24.2735	0.1709	3.6638	47.5	3.6319	(012)
	33.5043	0.2849	2.6725	29.1	2.6660	(104)
	36.0114	0.2279	2.4920	36.7	2.4804	(110)
	50.1425	0.3419	1.8178	25.7	1.8159	(024)
	54.7009	0.3419	1.6766	26.2	1.6732	(116)

Atomic force microscope images for Cr_2O_3 thin films at different

annealing temperature samples were illustrated in Fig. 4.

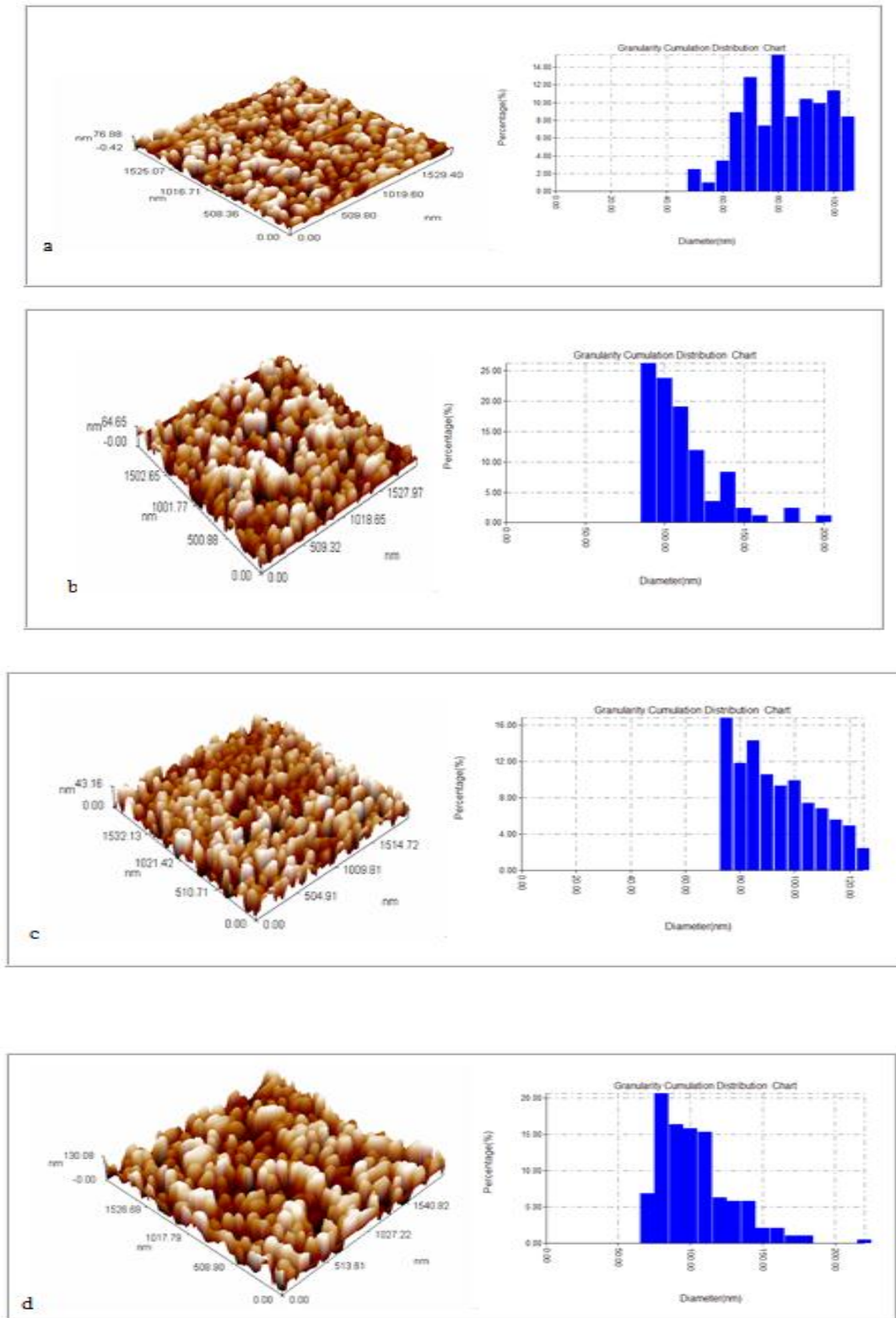


Fig. 4: Atomic force microscopy for Cr_2O_3 thin films at different annealing temperature at a- RT, b-300 °C, c-400 °C and d-500 °C.

The data collected for those samples from AFM images which are listed in Table 3 are revealed the three dimensional views watch give the grain size, average diameter and

average roughness which (is different between the highest point and the lowest point on the film) for Cr_2O_3 thin films at different annealing temperature. It could be seen how the

surface of the samples vary with different temperatures, grains with different shapes and diameters are appear in the surface. for $T_a = 400\text{ }^\circ\text{C}$, the surface becomes smoother with a Average Roughness of the order of 10.2 nm with a noticeable absence of the craters and rod-like features that appear at lower room temperature. Instead, regular crystallites with a typical lateral size of ~ 90.82 nm are observed, thereby indicating the

occurrence of an oriented crystalline growth of Cr_2O_3 on the glass substrate.

Atomic Force Microscope images of Cr_2O_3 thin films which is in a good agreement with structural properties from XRD analysis Table 2 illustrates increase in average diameter with increasing annealing temperature from RT to $(500)\text{ }^\circ\text{C}$, while the annealing film by $500\text{ }^\circ\text{C}$ have maximum values of Average Roughness and average r.m.s roughness value, (27 nm) and (32 nm), respectively.

Table 3: Average grains diameter, root mean square, and average roughness for Cr_2O_3 thin films at different annealing temperature.

T_a ($^\circ\text{C}$)	Average Roughness(nm)	Root mean square (nm)	Average grain diameter (nm)
RT	16.5	19.5	80.04
300	14.5	17	106.29
400	10.2	11.9	90.82
500	27	32	98.39

2. Optical studies

Ultraviolet absorption is a process in which the outer electrons of atoms or molecules absorb radiant energy and undergo transitions to high energy levels. The optical properties of a material describe how the characteristics of light are affected when it passes through it. Study of optical properties of thin films generally focuses on the energy gap

(E_g). A film is not just composed of perfect bulk material separated by grain boundaries; it also includes defects like unwanted impurities, stoichiometry deviations, point defects. The transmittance spectra for Cr_2O_3 films on glass substrate with different annealing temperature were carried out in the wavelength range 300–1100 nm at room temperature and shown in Fig. 5.

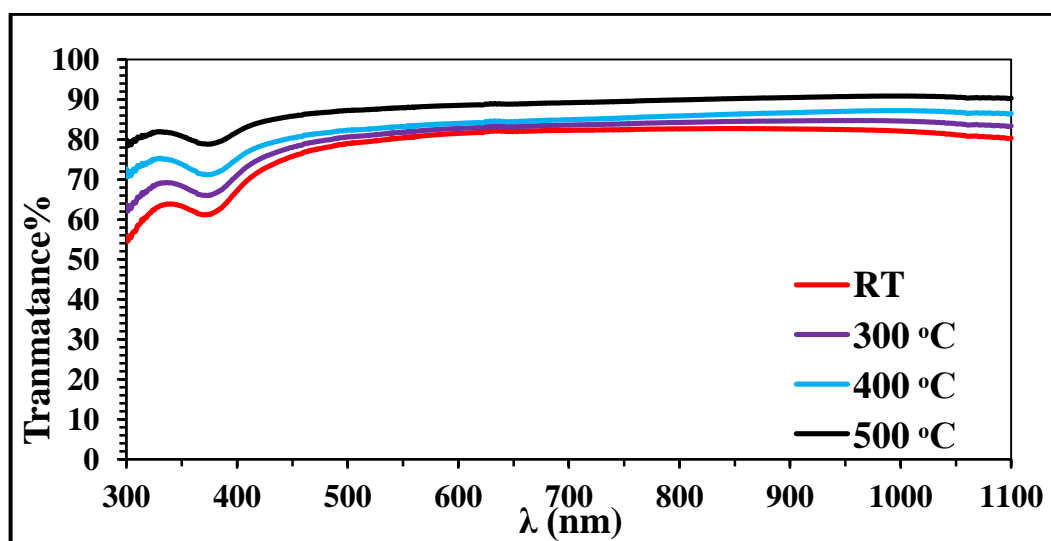


Fig. 5: The transmittance of the Cr_2O_3 film annealed at different annealing temperature.

It is evident that the optical transmittance increases in the visible region with increasing annealing temperature.

The absorption coefficient of the annealed Cr₂O₃ film can be calculated by a simple method from absorption spectra. The absorption coefficient, α (λ), is defined as [7]:

$$\alpha(\lambda) = 2.303A/t \tag{2}$$

where (A) is the absorbance and (t) is the film thickness.

Results are shown in Fig. 6. The absorption coefficient decreases with the increasing of the wavelength, note that the absorption coefficient changes slightly towards high wavelengths and

absorption coefficient begins to increase rapidly near the edge ($\lambda=380$ nm) of the optical absorption reflecting a direct electronic transitions within this range of wavelengths. For a given wavelength, the absorption coefficient increases with decreasing the annealing temperature might be due to the increasing regularity of crystalline granules and increased its size and give the opportunity for small grain to grow by removing barriers or granular boundary. The figure show have two band, one in UV region ,and the other in visible region which is called Q-band at the range about (330-430) nm.

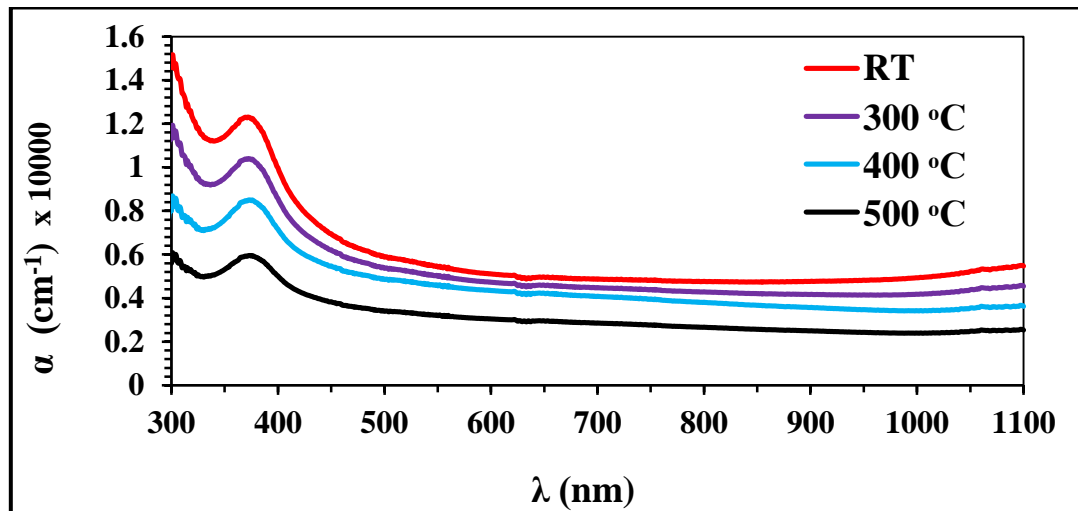


Fig. 6: Absorption coefficient as a function of the wavelength for the Cr₂O₃ film at different annealing temperature.

The optical energy gap values (E_g) for Cr₂O₃ thin films on glass have been determined by using equation [8].

$$\alpha h\nu = A(h\nu - E_g)^f \tag{3}$$

The plot of $(\alpha h\nu)^2$ against photon energy of thin film as shown in Fig. 7. The observed values of the optical

energy gap are increase with increasing annealing temperature. This means that annealing led to the absorption edge shift toward high energies near the levels of conduction band which are filled with electrons so the electrons need more energy and made energy gap seems to increase [9, 10].

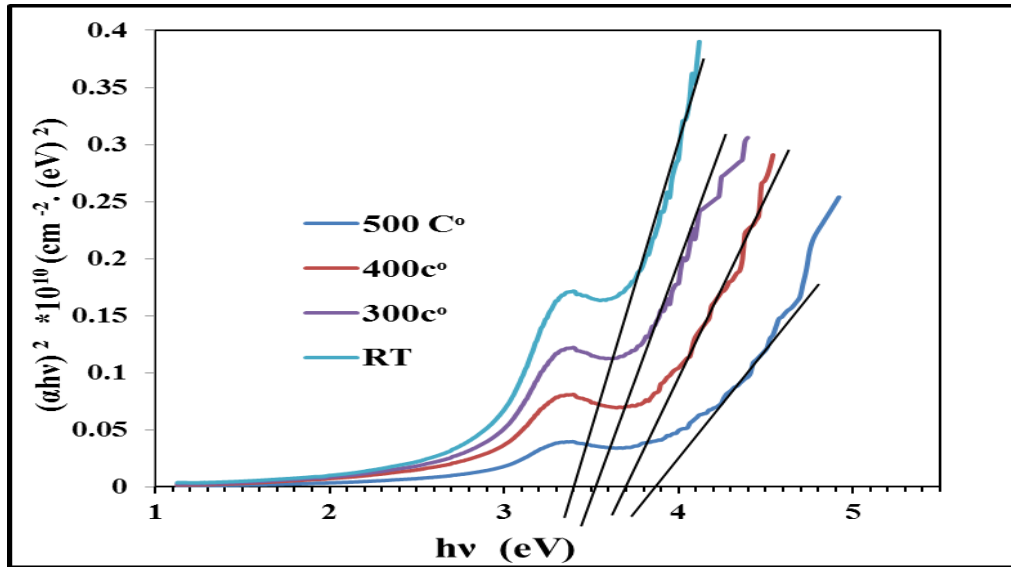


Fig. 7: Variation of the $(\alpha hv)^2$ vs. photon energy (hv) for Cr_2O_3 films.

The refractive index is an important parameter for optical materials and applications. The index of refraction for as deposited and annealed Cr_2O_3 films was estimated from the reflectance (R) data using the relation [9, 10]:

$$n = [4R / (R-1)^2 - k^2]^{1/2} - [(R+1)/(R-1)] \quad (4)$$

Fig. 8 shows the dependence of the refractive indices of Cr_2O_3 films as a function of wavelength.

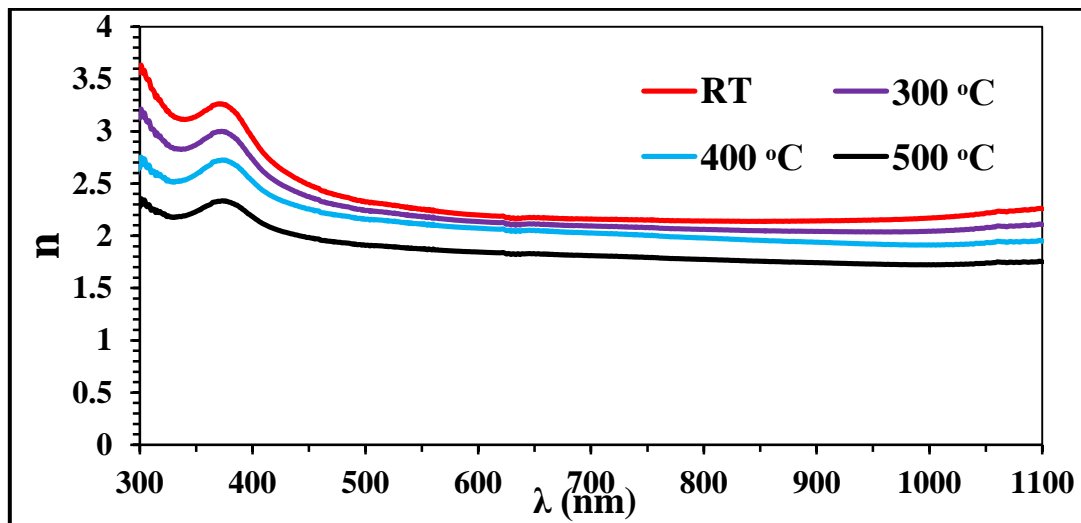


Fig. 8: The refractive indices of Cr_2O_3 films at different annealing temperature as a function of the wavelength.

It can be seen that the refractive index decreases with the increasing of wavelength, i.e. anomalous dispersion. This behavior is due to the increasing in energy gap. The variation refractive indices in the visible and ultraviolet region with increasing annealing temperature can be

attributed to the variation of optical absorption in the visible region and ultraviolet region after annealing.

It is known that extinction coefficient and absorption coefficient can be related by [4]:

$$K = \alpha \lambda / 4\pi \quad (5)$$

From Fig. 9 one can easily obtain the extinction coefficient of Cr₂O₃ films. The extinction coefficient depends mainly on absorption coefficient; for this reason, the

behavior of it is similar for absorption coefficient. It can be seen that the extinction coefficient decreases as the annealing temperature increase.

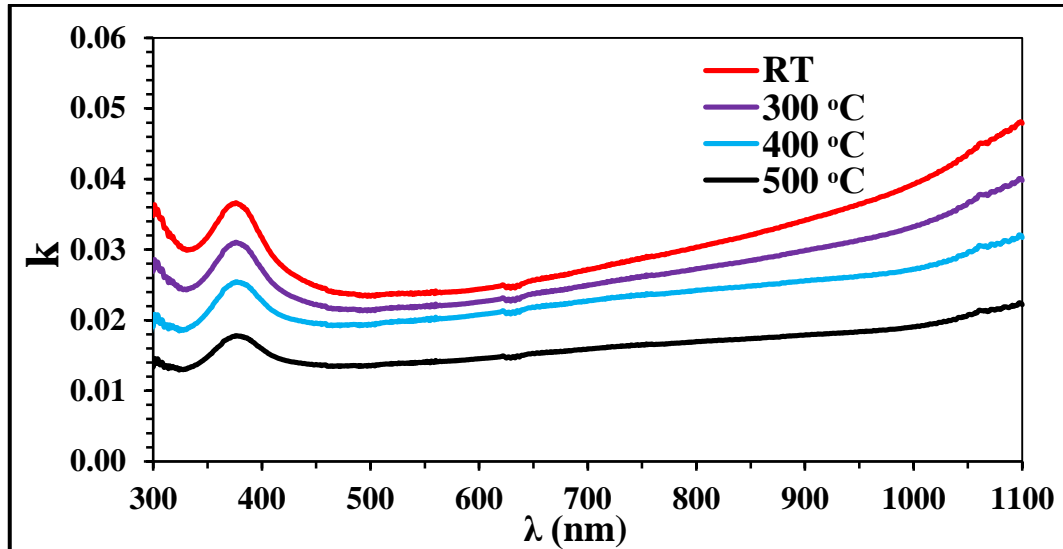


Fig. 9: The extinction coefficient of Cr₂O₃ films as a function of the wavelength prepared at different annealing temperature.

The dielectric constant can be defined as [11]:

$$\epsilon = \epsilon_r + i\epsilon_i \tag{6}$$

The real (ϵ_r) and imaginary (ϵ_i) parts of the dielectric constant are related to the n (refractive index) and k (extinction coefficient) values. These values can be calculated using the following formulas [12]:

$$\epsilon_r = n^2 - k^2 \tag{7}$$

$$\epsilon_i = 2nk \tag{8}$$

Figs. 10 and 11 present the dependence of the dielectric constant of the Cr₂O₃ films on the wavelength. The real and imaginary parts follow the same pattern and the values of real part are higher than imaginary part.

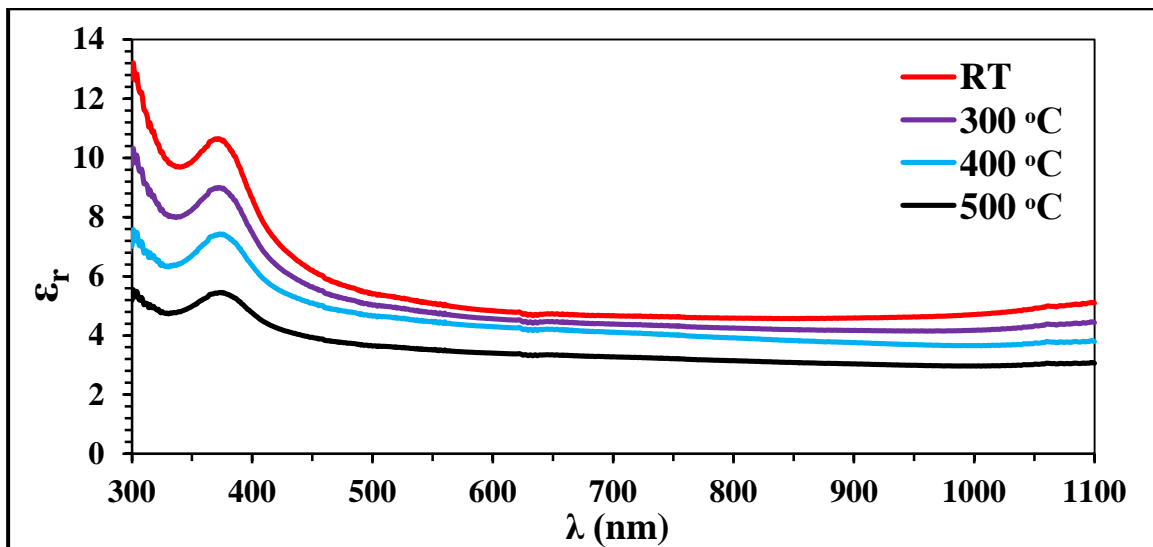


Fig. 10: The real part of dielectric constant of the Cr₂O₃ films as a function of wavelength.

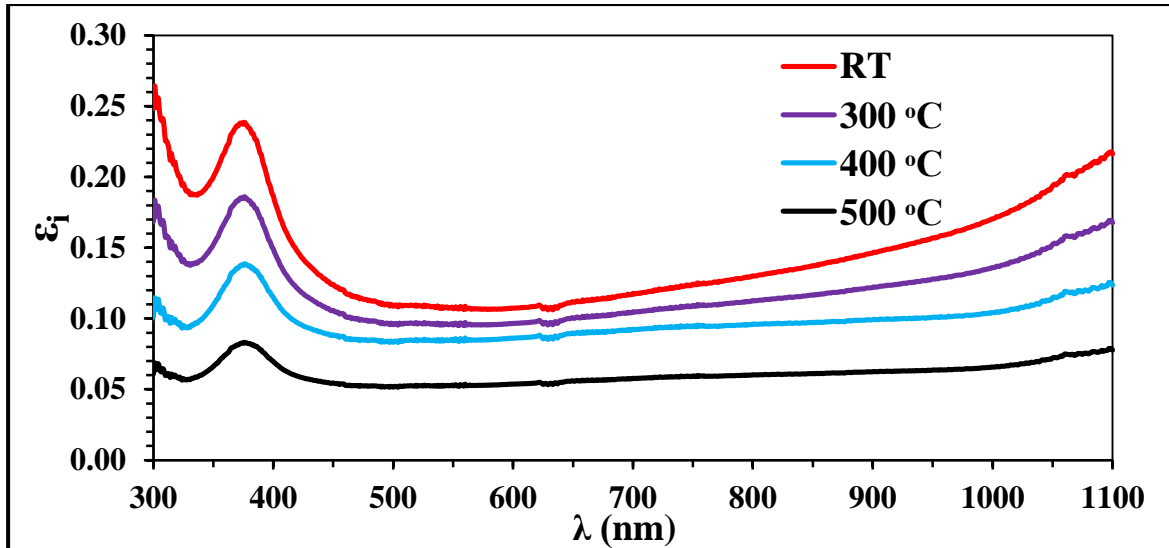


Fig. 11: The imaginary part of dielectric constant of the Cr₂O₃ films as a function of wavelength.

It can be seen that the real and imaginary parts of the dielectric constant decreases with increasing wavelength. On the other hand both of them are decreases with increasing annealing temperature. The variation of the dielectric constant depends on the value of the refractive index. By

contrast, the dielectric loss depends mainly on the extinction coefficient values which are related to the variation of absorption. In Table 4 the optical parameter of Cr₂O₃ (T%, α , K, n, ϵ_r , ϵ_i , E_g) and different annealing temperature at $\lambda=500$ nm.

Table 4: The values of T%, α , K, n, ϵ_r , ϵ_i , E_g at different annealing temperature at $\lambda=500$ nm

T _a (°C)	T%	α (cm ⁻¹)	K	n	ϵ_r	ϵ_i	E _g (eV)
RT	79.05	5876	0.023	2.323	5.394	0.109	3.4
300	80.70	5362	0.021	2.240	5.017	0.096	3.5
400	82.37	4848	0.019	2.156	4.648	0.083	3.7
500	87.31	3393	0.014	1.908	3.639	0.052	3.85

Conclusions

The deposited films of chromium oxide were thermodynamically stable at temperatures higher than 500 °C and this result is in a good agreement with previous results. The outcome of this investigation can be summarized as follows

-X-ray diffraction (XRD) study shows that Cr₂O₃ thin films are amorphous in nature.

-The transmittance increases with decreasing of annealing temperature

- The energy gap increases from 3.4 to 3.85 eV with increasing annealing temperatures and found to increase with increasing crystallite size.

- The optical constants values (α , k, n, ϵ_r and ϵ_i) decrease with increases annealing temperature

- The value of refractive index lies within 1.9 to 2.3 in the studied spectral range. Appreciable order of integrated optical quantities suggests that this material is a potential candidate for the application in selective surface devices.

References

- [1] G. Balakrishnan, P. Kuppusami, T. N. Sairam, R. V. S. Rao. *Surf. Eng.*, 25, October (2009) 223-227.
- [2] P. M. Sousa, A. J. Silvestre, N. Popovici, O. Conde, Elsevier, 247 (2005) 423-428.
- [3] M. M. Abdullah, F. M. Rajab, S. M. Al-Abbas, *AIP Adv.*, 1. 4, 2 (2014) 27121-2-11.
- [4] S. F. Oboudi and N. F. Habubi, *Baghdad Sci. J.*, 8, 2 (2011) 561-565.
- [5] H.M. Smith and A.F. Turner, *Appl. Optic.*, 1. 4 (1965) 147.
- [6] S. A. Maki and H. K. Al-attabi *J. KUFA – Phys*, 3, 1 (2011) 26-37.
- [7] B. N., K. Z. C. Madi, M. Tabbal, T. Christidis, S. Isber, *J. Phys. Conf. Ser*, 59, May (2007) 600-604.
- [8] G. K. Mohanapandiana and A. Krishnanb, College, *Int. J. Adv. Eng. Technol.* E-ISSN 097, April (2016) 273-279.
- [9] J. Tauc, in: J. Tauc (Ed.), *Amorphous and Liquid Semiconductors*, Plenum Press, New York, 1979, p. 159
- [10] T. Jantson, T. Avarmaa, T. Uustare, R. Jaaniso, *Sensors and Actuators B* 109, April (2005) 24-31.
- [11] A. Materials *J. Optoelectron. Adv. Mater.*, 13, May (2011) 485-490.
- [12] A. Hassena, S. El-Sayeda, W.M. Morsic, A.M. El Sayed, *Journal of Advances in Physics*, 3, 4 (2014) 571-584.